

Supplementary Information:

Predicting secondary structure propensities in IDPs
using simple statistics from three-residue fragments

Alejandro Estaña^{a,b}, Amélie Barozet^a, Assia Mouhand^b, Marc Vaisset^a,
Christophe Zanon^a, Pierre Fauret^a, Nathalie Sibille^b, Pau Bernadó^{b,*},
Juan Cortés^{a,*}

^a*LAAS-CNRS, Université de Toulouse, CNRS, Toulouse, France*

^b*Centre de Biochimie Structurale. INSERM, CNRS, Université de Montpellier, France*



*Corresponding authors

Email addresses: pau.bernado@cbs.cnrs.fr, juan.cortes@laas.fr

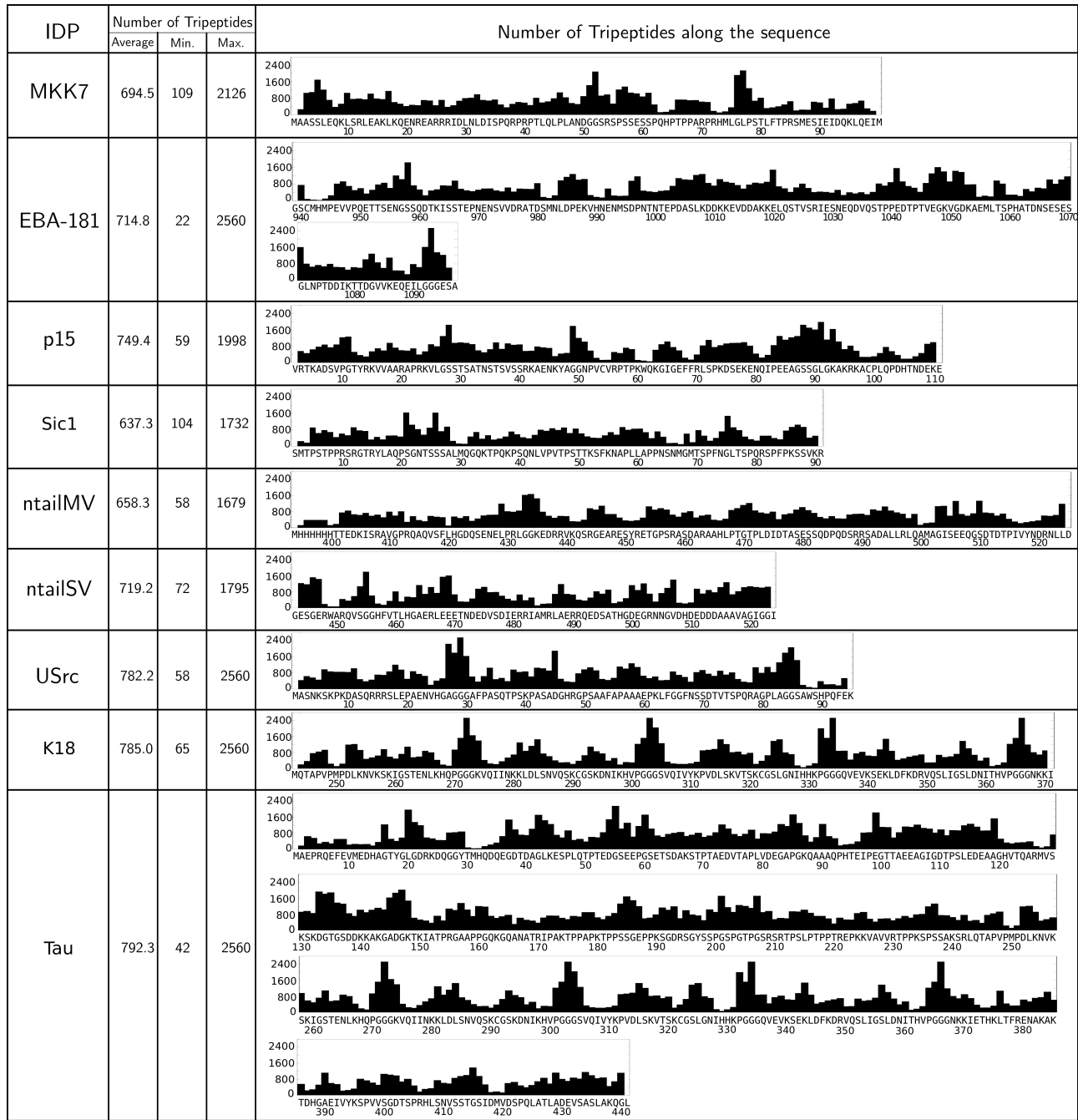


Figure S1: Number of structures in our database for the tripeptides in the nine studied IDPs. The value for each tripeptide is shown on the central residue.

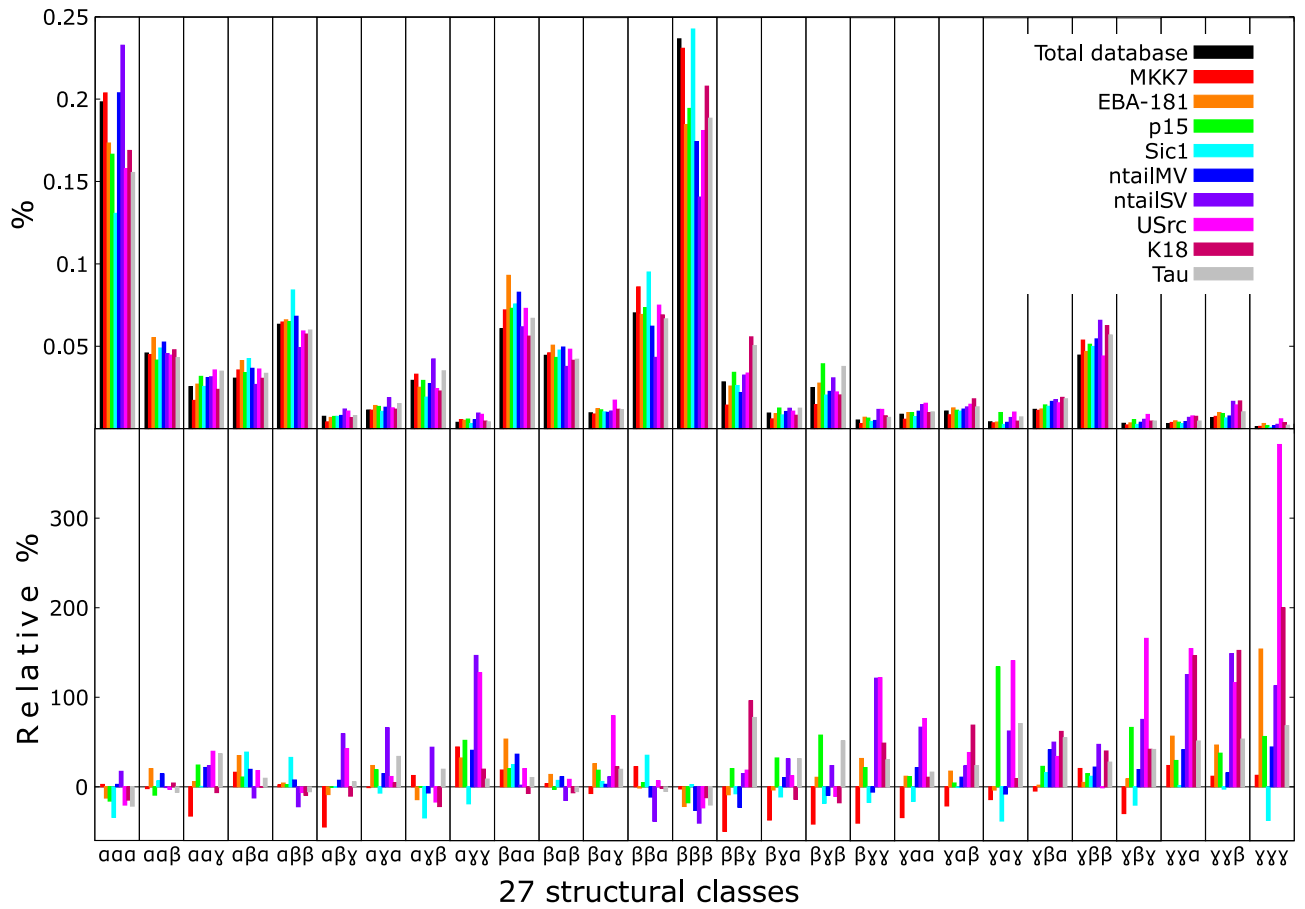


Figure S2: (Top) Percentage of each secondary structure class for the tripeptides in the entire database and for the subset of tripeptides of the nine IDPs considered in this study. (Bottom) Relative percentage for each each structural class in all IDPs compared with the entire database.

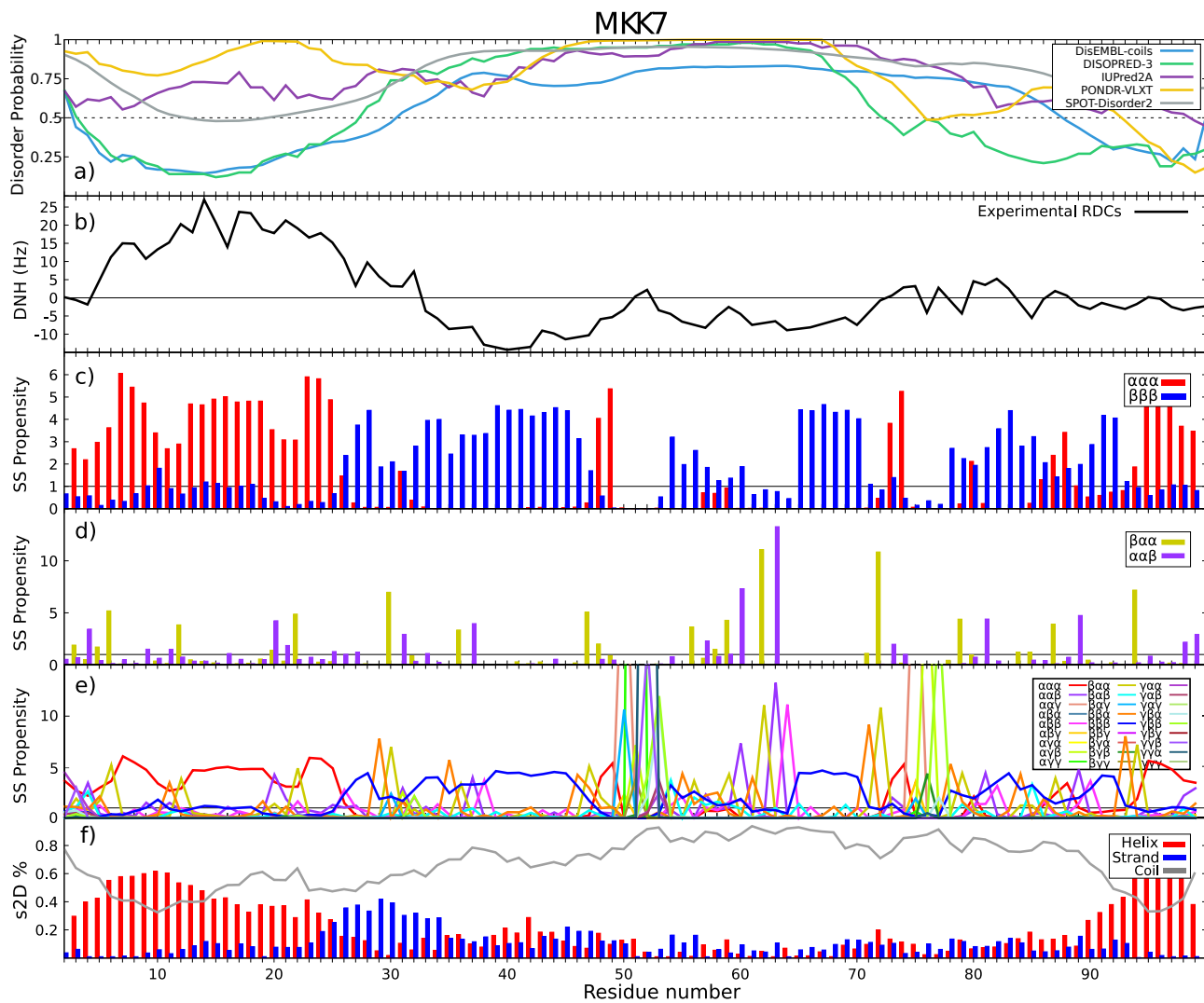


Figure S3: LS2P secondary structure prediction for MKK7. (a) Disorder probability predictions. (b) Experimental RDC profile. (c) Helical ($\alpha\alpha\alpha$) and extended ($\beta\beta\beta$) propensities predicted by LS2P. (d) $\beta\alpha\alpha$ and $\alpha\alpha\beta$ propensities predicted by LS2P, allowing to identify β -turns. (e) Propensities predicted by LS2P for the 27 structural classes. For clarity purposes, values are truncated at 15. (f) Secondary structure populations predicted by s2D.

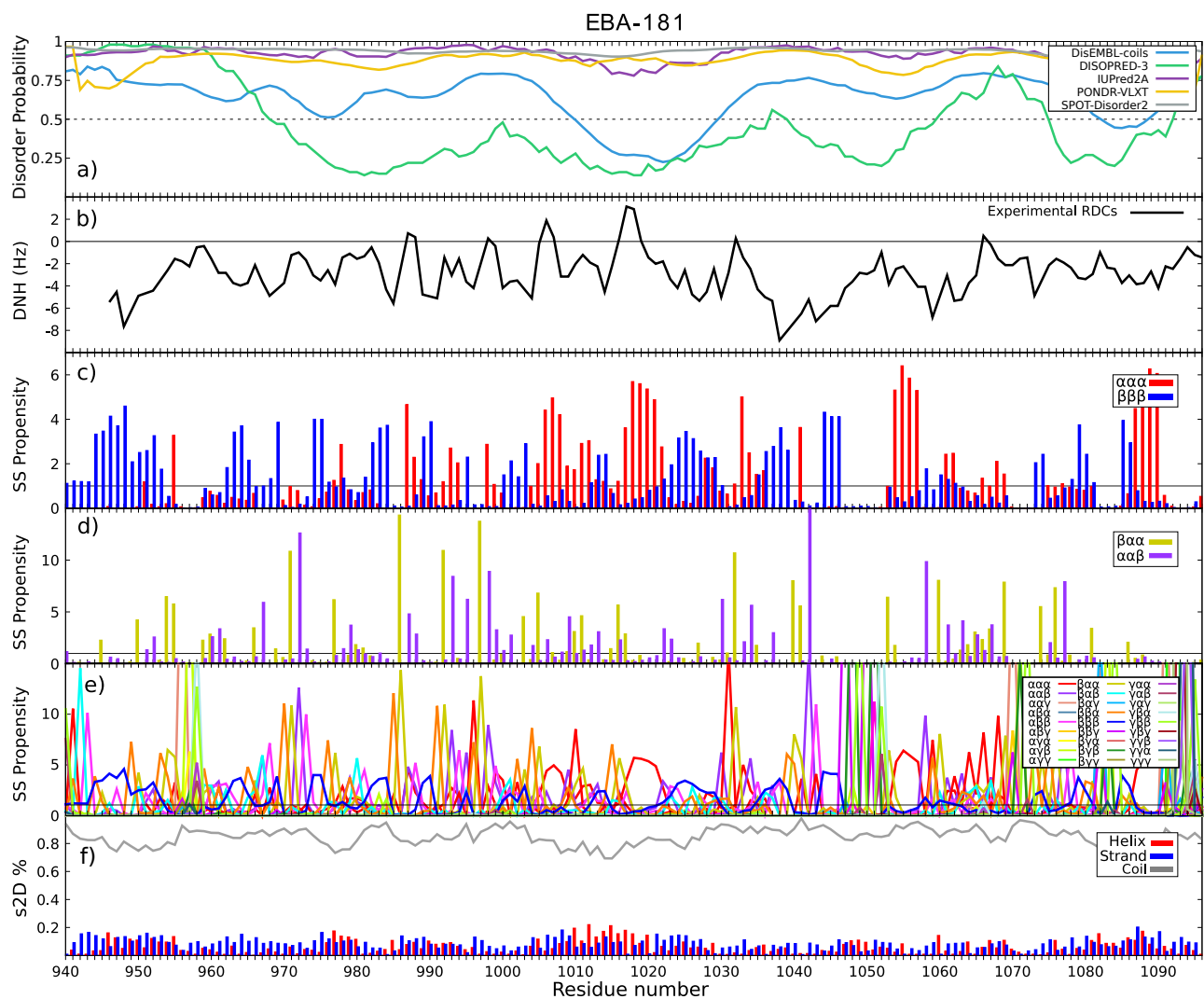


Figure S 4: LS2P secondary structure prediction for EBA-181. (a) Disorder probability predictions. (b) Experimental RDC profile. (c) Helical ($\alpha\alpha\alpha$) and extended ($\beta\beta\beta$) propensities predicted by LS2P. (d) $\beta\alpha\alpha$ and $\alpha\alpha\beta$ propensities predicted by LS2P, allowing to identify β -turns. (e) Propensities predicted by LS2P for the 27 structural classes. For clarity purposes, values are truncated at 15. (f) Secondary structure populations predicted by s2D.

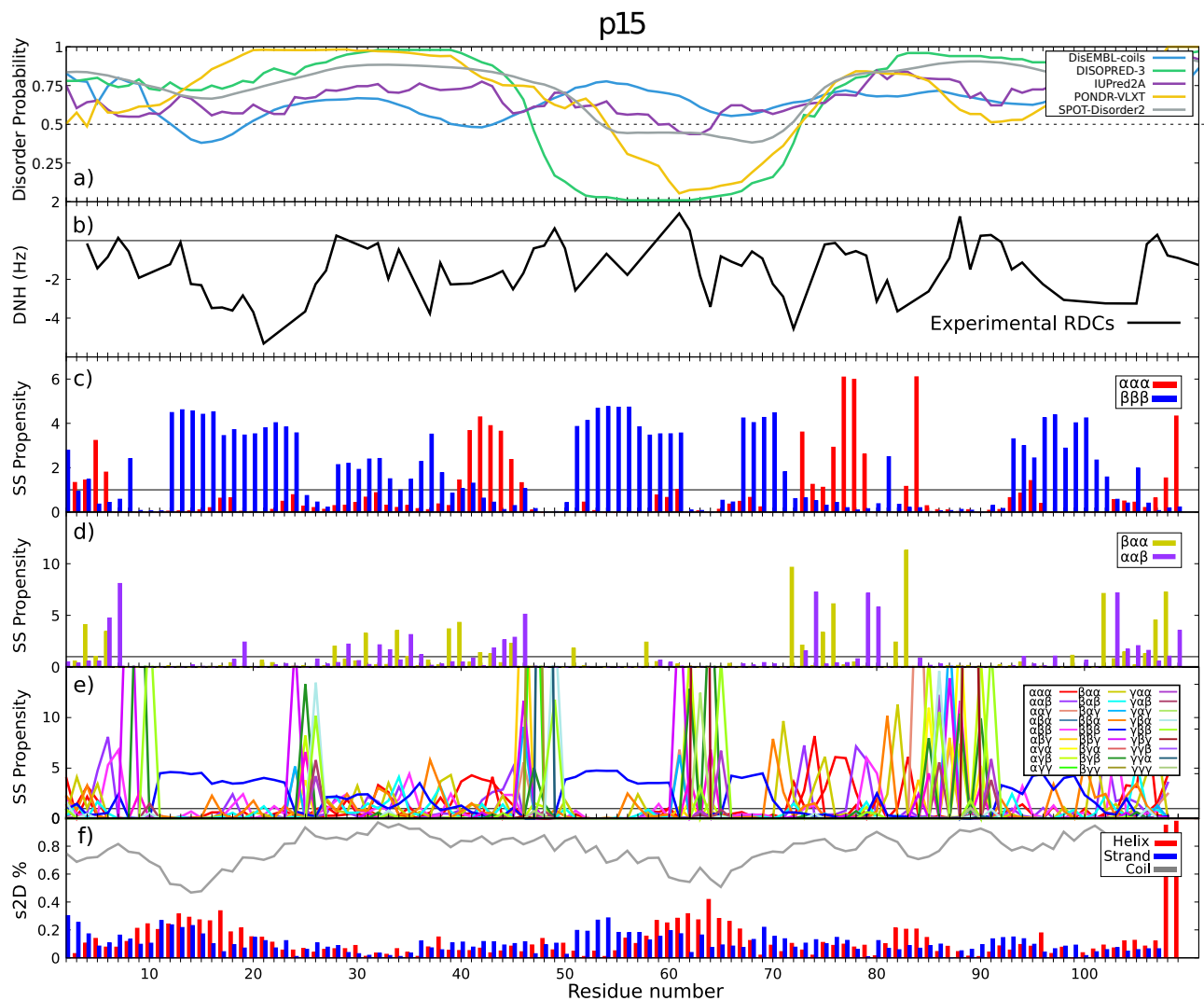


Figure S5: LS2P secondary structure prediction for p15. (a) Disorder probability predictions. (b) Experimental RDC profile. (c) Helical ($\alpha\alpha\alpha$) and extended ($\beta\beta\beta$) propensities predicted by LS2P. (d) $\beta\alpha\alpha$ and $\alpha\alpha\beta$ propensities predicted by LS2P, allowing to identify β -turns. (e) Propensities predicted by LS2P for the 27 structural classes. For clarity purposes, values are truncated at 15. (f) Secondary structure populations predicted by s2D.

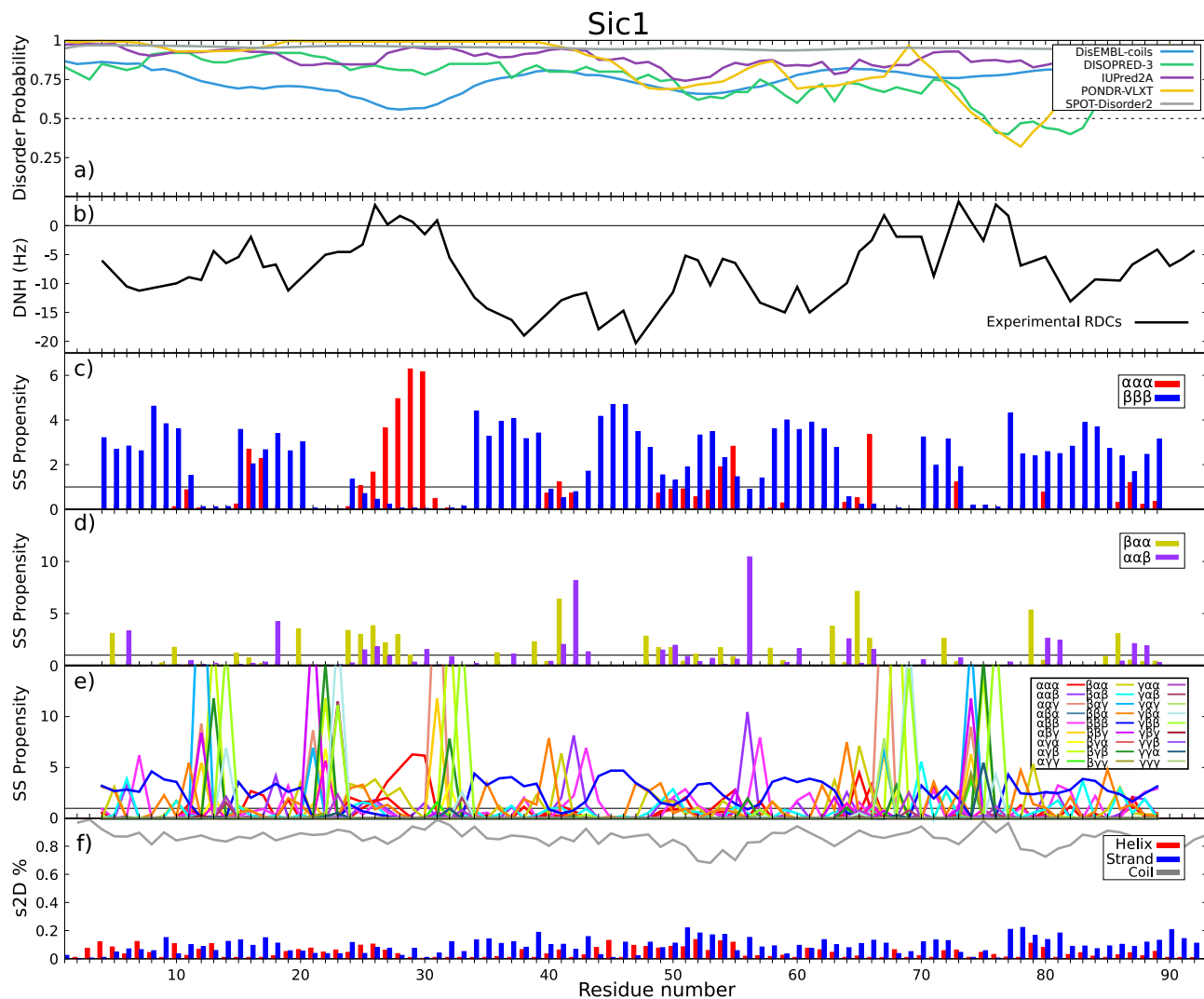


Figure S6: LS2P secondary structure prediction for Sic1. (a) Disorder probability predictions. (b) Experimental RDC profile. (c) Helical ($\alpha\alpha\alpha$) and extended ($\beta\beta\beta$) propensities predicted by LS2P. (d) $\beta\alpha\alpha$ and $\alpha\alpha\beta$ propensities predicted by LS2P, allowing to identify β -turns. (e) Propensities predicted by LS2P for the 27 structural classes. For clarity purposes, values are truncated at 15. (f) Secondary structure populations predicted by s2D.

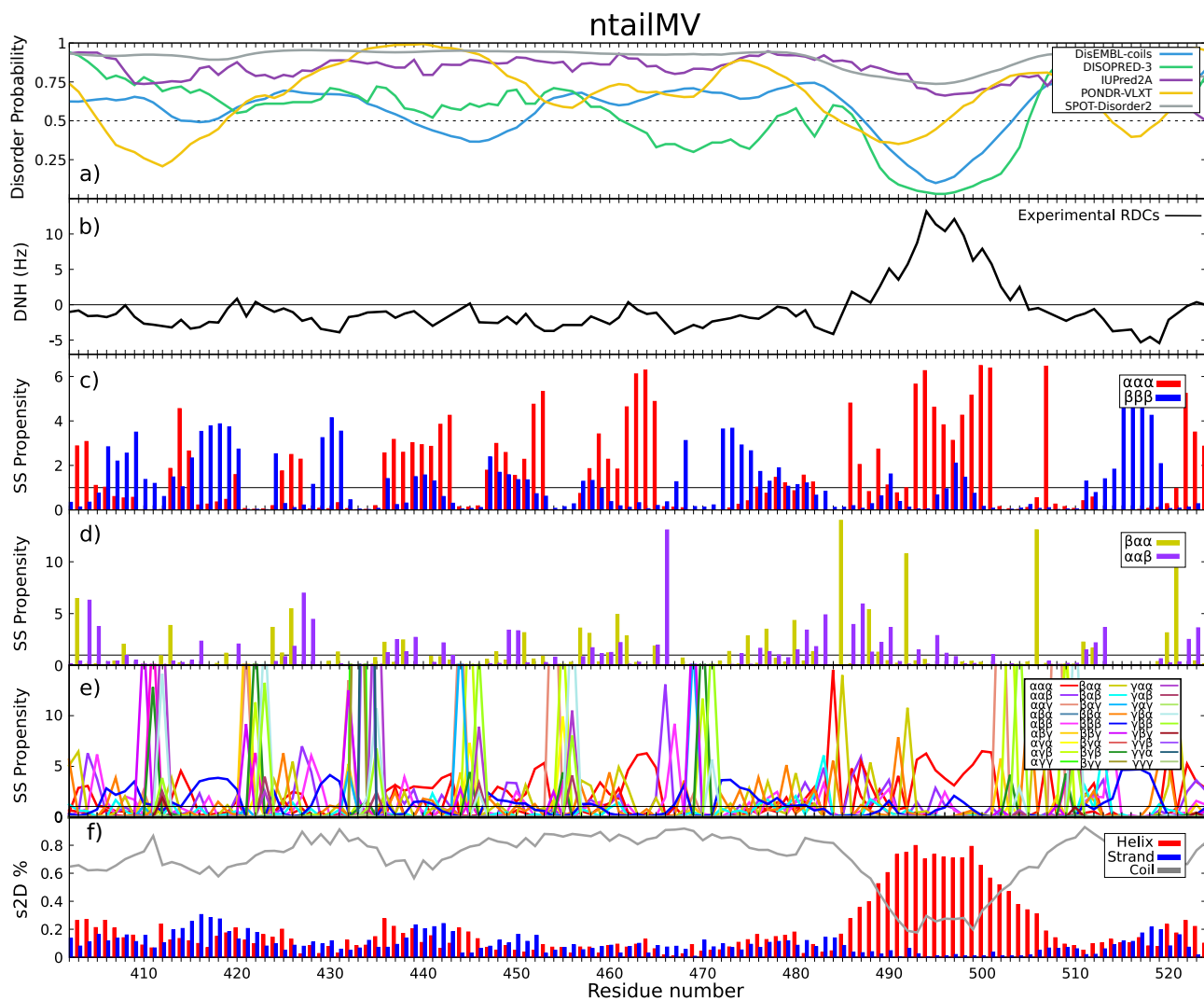


Figure S7: LS2P secondary structure prediction for ntailMV. (a) Disorder probability predictions. (b) Experimental RDC profile. (c) Helical ($\alpha\alpha\alpha$) and extended ($\beta\beta\beta$) propensities predicted by LS2P. (d) $\beta\alpha\alpha$ and $\alpha\alpha\beta$ propensities predicted by LS2P, allowing to identify β -turns. (e) Propensities predicted by LS2P for the 27 structural classes. For clarity purposes, values are truncated at 15. (f) Secondary structure populations predicted by s2D.

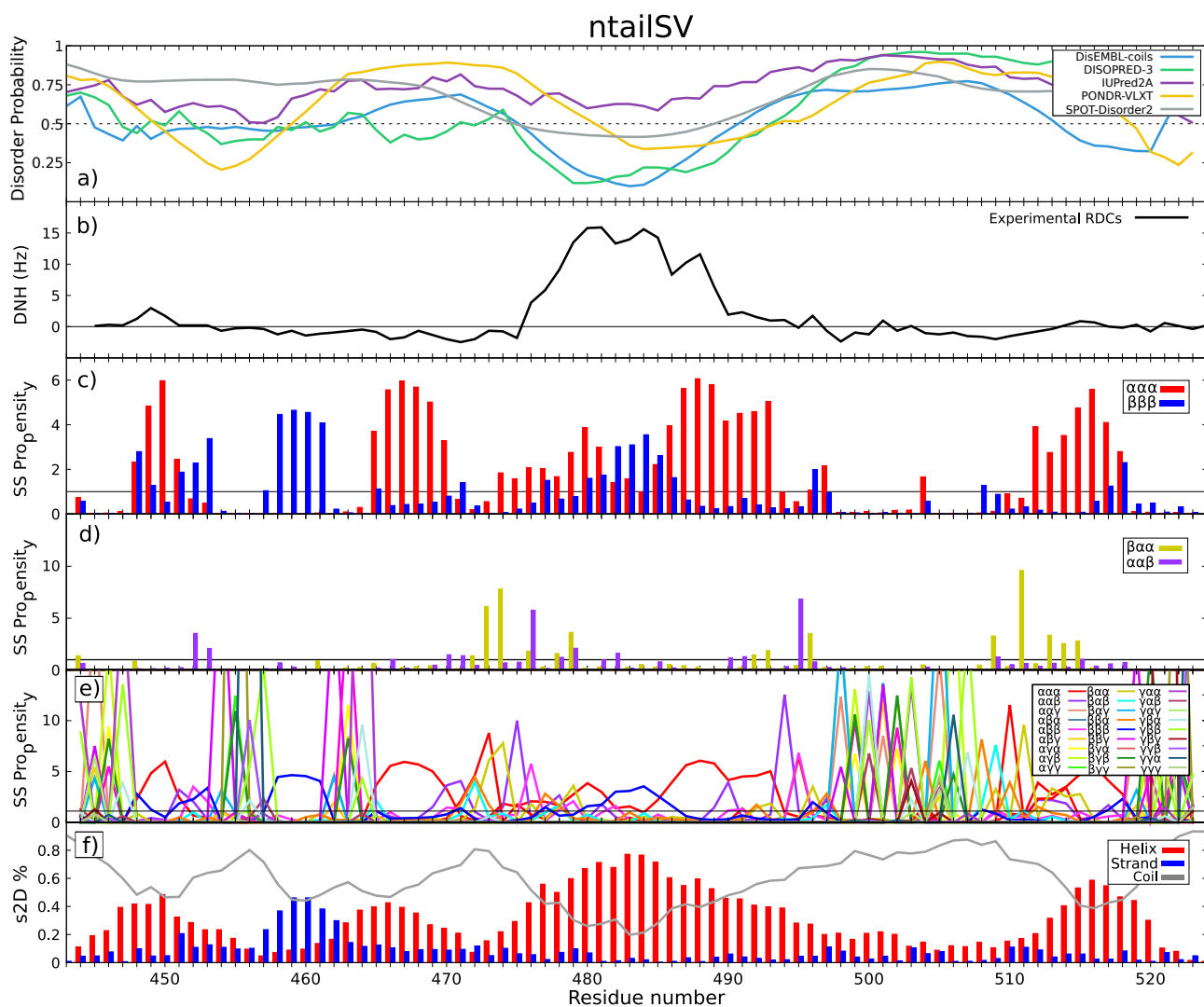


Figure S 8: LS2P secondary structure prediction for ntailSV. (a) Disorder probability predictions. (b) Experimental RDC profile. (c) Helical ($\alpha\alpha\alpha$) and extended ($\beta\beta\beta$) propensities predicted by LS2P. (d) $\beta\alpha\alpha$ and $\alpha\alpha\beta$ propensities predicted by LS2P, allowing to identify β -turns. (e) Propensities predicted by LS2P for the 27 structural classes. For clarity purposes, values are truncated at 15. (f) Secondary structure populations predicted by s2D.

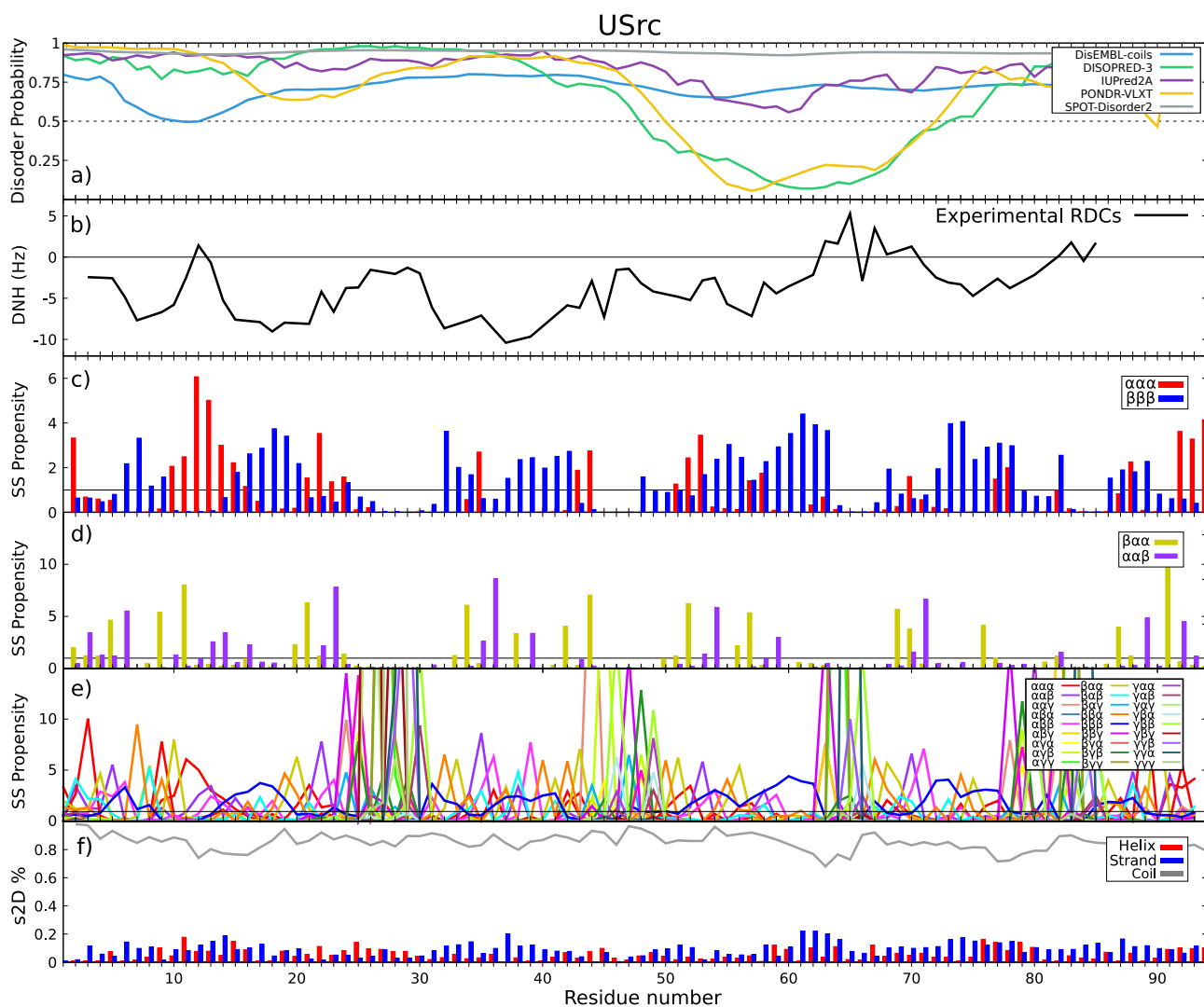


Figure S9: LS2P secondary structure prediction for USrc. (a) Disorder probability predictions. (b) Experimental RDC profile. (c) Helical ($\alpha\alpha\alpha$) and extended ($\beta\beta\beta$) propensities predicted by LS2P. (d) $\beta\alpha\alpha$ and $\alpha\alpha\beta$ propensities predicted by LS2P, allowing to identify β -turns. (e) Propensities predicted by LS2P for the 27 structural classes. For clarity purposes, values are truncated at 15. (f) Secondary structure populations predicted by s2D.

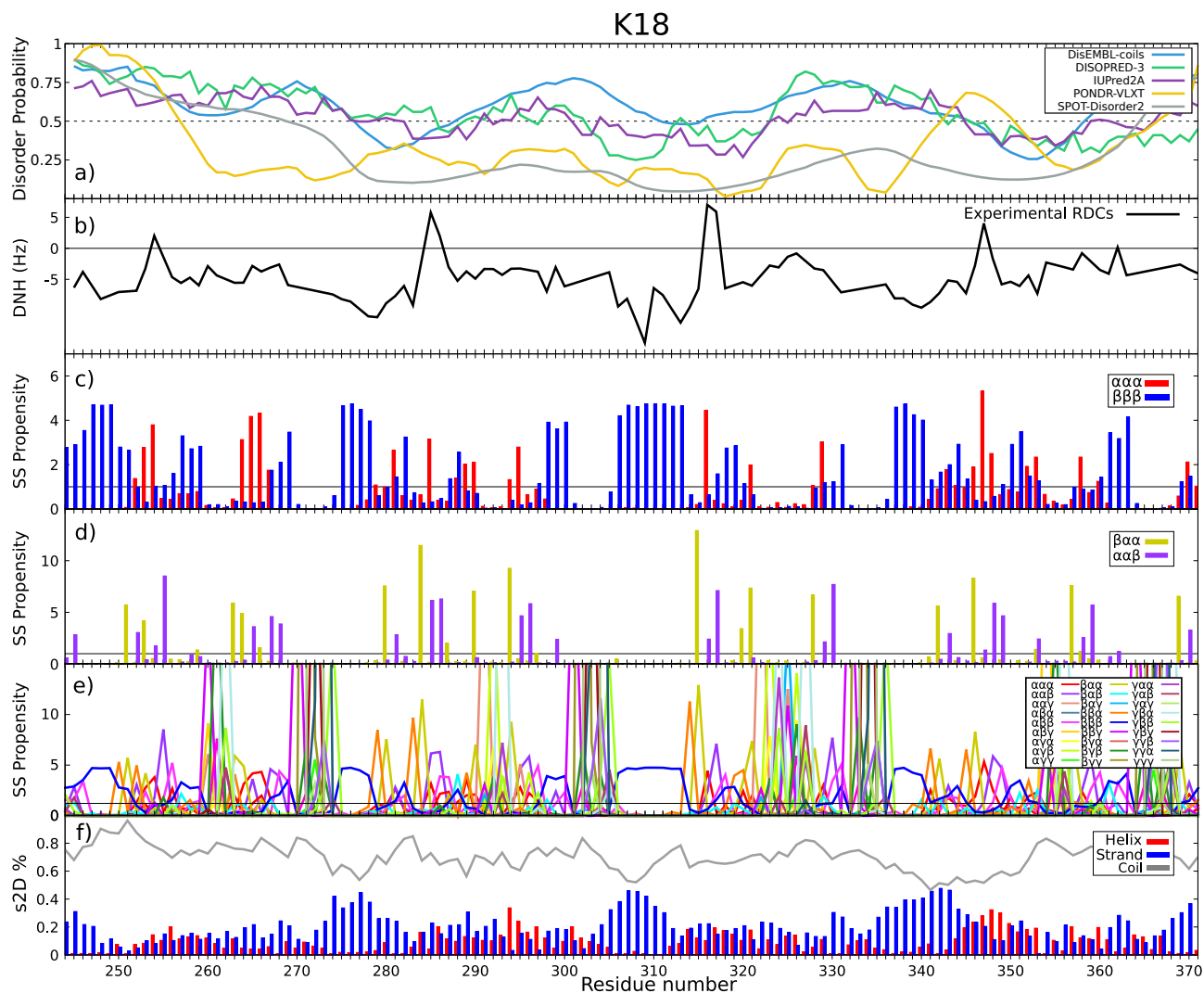


Figure S10: LS2P secondary structure prediction for K18. (a) Disorder probability predictions. (b) Experimental RDC profile. (c) Helical ($\alpha\alpha\alpha$) and extended ($\beta\beta\beta$) propensities predicted by LS2P. (d) $\beta\alpha\alpha$ and $\alpha\alpha\beta$ propensities predicted by LS2P, allowing to identify β -turns. (e) Propensities predicted by LS2P for the 27 structural classes. For clarity purposes, values are truncated at 15. (f) Secondary structure populations predicted by s2D.

